Effect of the Headgroup Structure on the Aggregation Behavior and Stability of Self-Assemblies of Sodium *N*-[4-(*n*-Dodecyloxy)benzoyl]-L-aminoacidates in Water

Ashok Mohanty and Joykrishna Dey*

Department of Chemistry, Indian Institute of Technology, Kharagpur-721 302, India

Received August 26, 2006. In Final Form: October 25, 2006

Three amino acid-derived chiral surfactants, sodium *N*-[4-(*n*-dodecyloxy)benzoyl]-L-leucinate (SDBL), sodium *N*-[4-(*n*-dodecyloxy)benzoyl]-L-isoleucinate (SDBIL), and sodium *N*-[4-(*n*-dodecyloxy)benzoyl]-L-threoninate (SDBT), were synthesized, and their aggregation behavior was studied in aqueous solution. Surface tension, fluorescence probe, dynamic light scattering, nuclear magnetic resonance (NMR), gel permeation chromatography, circular dichroism, and optical as well as transmission electron microscopic techniques were utilized to characterize the self-assemblies formed by the amphiphiles. Results of these studies reveal that the surfactants have a very low critical aggregation concentration (cac) and they form spherical vesicles spontaneously in dilute aqueous solution. The mean diameters of the vesicles were measured to be in the range of 130−190 nm. ^{1}H NMR spectra indicated hydrogen bonding between the amide groups near the surfactant headgroup, which is one of the driving forces for vesicle formation. The vesicle formation is more favored at a pH of about 7.0. The amphiphiles also form chiral helical aggregates at relatively higher concentrations as indicated by circular dichroism spectra. The stability of the vesicles was also evaluated with respect to the surfactant concentration, pH, temperature, and aging. The vesicles have a tendency to transform into elongated vesicles (closed tubules) or rodlike micelles with an increase of the surfactant concentration and/or pH. On the basis of the results obtained from different studies, phase diagrams for all three water/amphiphile systems have been constructed. The studies have further shown that the stereogenic center at the amino acid side chain has a significant effect on the aggregation properties of the amphiphiles and on the stability of the self-assemblies.

Introduction

The synthesis and study of the aggregation behavior of surfactants has been a subject of research interest in recent years because of their utility in wide-ranging chemical and technological areas such as organic, analytical, and physical chemistry, biochemistry, pharmaceuticals, petroleum recovery, detergents, cosmetics, paints and coatings, mineral processing, and food science.[1] *N*-Acylamino acid surfactants (NAASs), particularly, have received considerable attention because they are mild, nonirritating to human skin, and easily biodegradable,[2] which make them suitable candidates for use as detergents, foaming agents, and shampoos. Another important feature of the NAASs is their chirality. Owing to their chirality, NAASs are used in stereoselective synthesis[3] and as chiral selectors in micellar electrokinetic chromatography (MEKC) for enantiomeric separations using capillary electrophoresis (CE).[4] Various NAASs have been synthesized and used in MEKC for enantiomeric separation of the racemates of a wide spectrum of compounds including small organic molecules, pesticides, herbicides, and drugs.[4] Besides their above-mentioned utilities, chiral NAASs also show some interesting aggregation behavior compared to achiral ones. For example, the optically active NAASs have a lower critical aggregation concentration (cac),[5] form different lyotropic liquid crystals,[6] and in some cases form different types of self-assembly morphology[7] compared to the racemic ones. One of the important effects of chirality is the enhanced lifetime of the aggregates.[8] There is a great demand for a thorough understanding of the effect of the molecular stereochemistry in the surfactant self-assembly in the field of biomedical research. This is because the chiral centers in biological lipids often control the nature of their self-assemblies under physiological conditions.[9] Also the nature of vesicular structures used for controlled drug delivery depends on the stereochemistry of the chiral amphiphile.[10]

The most common type of aggregate formed by the NAASs is the micelle. However, in some recent reports by others[11] as well as from this laboratory,[12] authors have shown the spontaneous formation of vesicles from single-tailed NAASs in aqueous solution. We have demonstrated the utility of the vesicle-forming NAAS sodium *N*-[4-(*n*-dodecyloxy)benzoyl]-L-valinate (SDBV)

* To whom correspondence should be addressed. Phone: 91-3222-283308. Fax: 91-3222-255303. E-mail: joydey@chem.iitkgp.ernet.in

(1) Fuhrhop, J. -H.; Helfrich, W. *Chem. Rev.* **1993**, *93*, 1565.
(2) (a) Takehara, M.; Moriyuki, H.; Yoshimura, I.; Yoshida, R. *J. Am. Oil Chem. Soc.* **1972**, *49*, 143. (b) Takehara, M. *Colloids Surf.* **1989**, *38*, 149.
(3) (a) Zhang, Y.; Sun, P. *Tetrahedron: Asymmetry* **1996**, *7*, 3055. (b) Zhang, Y.; Wu, W. *Tetrahedron: Asymmetry* **1999**, *8*, 3575. (c) Diego-Castro, M. J.; Hailes, H. C. *Chem. Commun.* **1998**, 1549.
(4) (a) Yrabe, H. H.; Shamsi, S. A.; Warner, I. M. *Anal. Chem.* **1999**, *71*, 3992. (b) Palmer, C. P. *Electrophoresis* **2000**, *21*, 4054. (c) Palmer, C. P.; Terabe, S. *Anal. Chem.* **1997**, *69*, 1852. (d) Shamsi, S. A.; Akbey, C.; Warner, I. M. *Anal. Chem.* **1998**, *70*, 3078. (e) Hayenes, J. L., III; Billot, E. J.; Yarabe, H. H.; Warner, I. M.; Shamsi, S. A. *Electrophoresis* **2000**, *21*, 1597.
(5) (a) Miyagishi, S.; Nishida, M. *J. Colloid Interface Sci.* **1978**, *65*, 380. (b) Miyagishi, S.; Higashide, M.; Asakawa, T.; Nishida, M. *Langmuir* **1991**, *7*, 51. (c) Takehara, M.; Yoshimura, I.; Yoshida, R. *J. Am. Oil Chem. Soc.* **1974**, *51*, 419.
(6) (a) Tracey, A.; Radley, K. *Langmuir* **1990**, *6*, 1221. (b) Tracey, A.; Radley, K. *J. Phys. Chem.* **1984**, *88*, 6044.
(7) Fuhrhop, J. H.; Schnieder, P.; Rosenberg, J.; Boekema, E. *J. Am. Chem. Soc.* **1987**, *109*, 3387.
(8) Morigaki, K.; Dallavalle, S.; Walde, P.; Colonna, S.; Luisi, P. L. *J. Am. Chem. Soc.* **1997**, *119*, 292.
(9) (a) Zarif, L.; Polidori, A.; Pucci, B.; Gulik-Krzywicki, T.; Pavia, A.; Reiss, J. *Chem. Phys. Lipids* **1996**, *79*, 165. (b) Hato, M.; Minamikawa, H. *Langmuir* **1996**, *12*, 1658.
(10) Jaeger, D.; Kubicz-Loring, E.; Price, R.; Nakagawa, H. *Langmuir* **1996**, *12*, 5803.
(11) (a)Wang, C.; Huang, J.; Tang, S.; Zhu, B. *Langmuir* **2001**, *17*, 6389. (b) Wang, C.; Gao, Q.; Huang, J. *Langmuir* **2003**, *19*, 3757. (c) Du, X.; Hlady, V. *J. Phys. Chem. B* **2002**, *106*, 7295.
(12) (a) Roy, S.; Dey, J. *Langmuir* **2005**, *21*, 10362. (b) Mohanty, A.; Dey, J. *Langmuir* **2004**, *20*, 8452. (c) Roy, S.; Dey, J. *Bull. Chem. Soc. Jpn.* **2006**, *79*, 59.

10.1021/la0625143 CCC: $37.00
Published on Web 12/06/2006

Chart 1. Molecular Structures of the Amphiphiles Studied

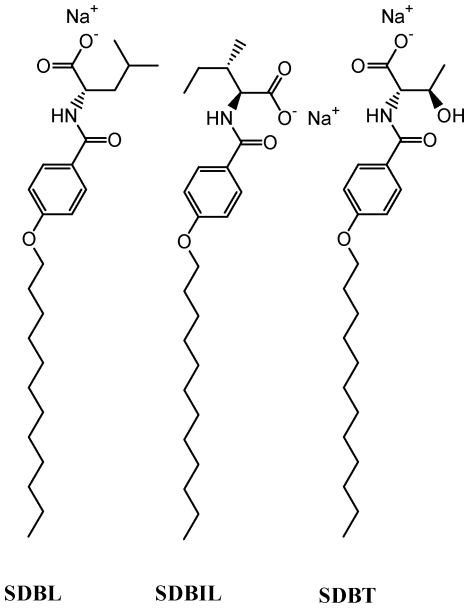

for enantiomeric separation of some selected chiral analytes using MEKC.[13] More recently, we have utilized other amphiphiles of the homologous series, i.e., sodium *N*-[4-(*n*-dodecyloxy)benzoyl]-L-leucinate (SDBL), -L-isoleucinate (SDBIL), and -L-threoninate (SDBT), for enantiomeric separations using MEKC and have observed that the chiral selectivities of these amphiphiles are significantly different from that of SDBV.[14] To explain the different chiral selectivities of these amphiphiles, we have undertaken this work of studying the aggregation behavior of the surfactants in aqueous solutions. The focus of the present work is to study the effects of the headgroup structure on the self-assembly properties of this class of amphiphiles (see Chart 1 for the molecular structures). Moreover, these amphiphiles being novel, the detail aggregation behavior study will open up opportunities for their use in other areas. Therefore, the objective of the present work is to study the aggregation behavior of the amphiphiles, which includes (i) determination of the cac, (ii) measurement of the size of the self-assemblies, (iii) study of the morphology of the self-assemblies, (iv) study of the microenvironments of the self-assemblies, (v) investigation of the effects of the concentration, solution pH, temperature, and aging on the self-assembly formation, and (vi) study of the effect of a stereogenic center at the amino acid side chain on the formation of chiral aggregates.

Results

Turbidity Studies. All three amphiphiles when dissolved in water produce clear solutions at pH ≥ 7.0. When the pH is lowered to 6.5−5.0, after 10−12 h of sample preparation, SDBL precipitates out of the solution as needle-like crystals, SDBIL forms fibrous structures like SDBV,[12b] and SDBT gives a clear solution. Thus, the three amphiphiles behave differently when the pH is varied in the acidic range. The fibrous aggregates (see Figure 1) formed by SDBIL are stable for more than 15 days of aging and become soluble when the temperature is raised to 60 °C but reappear when the temperature is lowered to room temperature (25 °C). At pH lower than 4.5 all the surfactants precipitate out of the solution. It is important to note that the

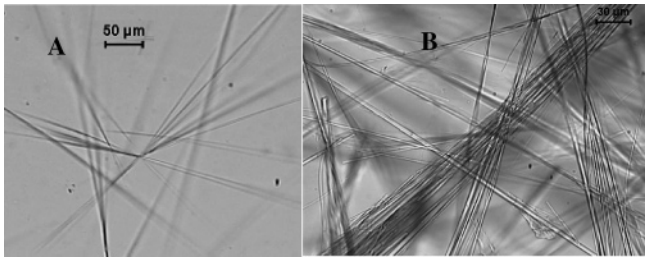

Figure 1. Optical micrographs of 0.125 mM SDBL (A) and SDBIL (B) in 20 mM phosphate buffer, pH 6.0, after 12 h of aging.

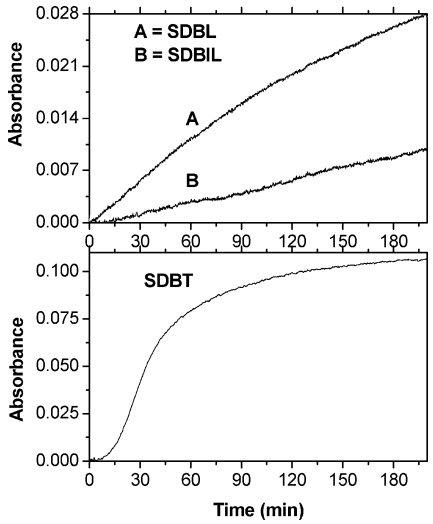

Figure 2. Time dependence of the absorbance of 1 mM SDBL, SDBIL, and SDBT in water (pH 7.5).

aqueous solution of the amphiphiles in the pH range 7.0−8.0 appears blue to the naked eye. This could be due to the light scattering properties of the large aggregates formed by the surfactant molecules in aqueous solution. In fact, a tailing of the band at 255 nm up to 500 nm was observed in the UV−vis spectra of 0.125 mM aqueous solutions (Figure S1 of the Supporting Information) of the amphiphiles, which was absent in methanol solution. The appearance of a blue color of the aqueous solution of the surfactants was also followed spectrophotometrically by measuring the time dependence of absorbance at 400 nm, where the surfactant has no absorbance. The plots of absorbance as a function of time for 1 mM SDBL, SDBIL, and SDBT (pH 7.5) are shown in Figure 2. As can be observed, absorbance increases with time, indicating an increase of the turbidity of the solution. The scattering is most pronounced in SDBT solution and least in the case of SDBIL. To investigate the effect of surfactant concentration and pH on the formation of large aggregates, a turbidity study was carried out for both concentrated (2 mM) and dilute (0.5 mM) solutions of the amphiphiles in water and in 0.1 M NaOH (see Figure S2 of the Supporting Information). It was observed that the aggregates grow faster in concentrated solutions compared to the dilute solution.

Critical Aggregation Concentration. The cac of the amphiphiles in water (pH 7.5) was determined by the surface tension measurement method following the reported procedure.[12] The cac values (see Table 1) were further determined by the fluorescence probe method using *N*-phenyl-1-naphthylamine (NPN) as the probe molecule. The fluorescence emission spectrum of NPN is known to exhibit a large blue shift with a concomitant

(13) (a) Mohanty, A.; Dey, J. *Chem. Commun.* **2003**, *12*, 1384. (b) Mohanty, A.; Dey, J. *J. Chromatogr., A* **2005**, *1070*, 185.
(14) Mohanty, A.; Dey, J. *J. Chromatogr., A* **2006**, *1128*, 259.

Table 1. Aggregation and Surface-Active Properties of the Amphiphiles SDBL, SDBIL, and SDBT

property	SDBL	SDBIL	SDBT
cac × 10^5 (M)	1.30, 1.90[a]	1.00, 1.60[a]	1.50, 2.00[a]
D_z (nm)	151	135	193
I_1/I_3	1.02	1.04	1.05
r	0.194	0.195	0.195
η (mPa s)	105.27[b]	110.61[b]	109.97
pK_a	6.40	6.30	6.20

[a] Values obtained from the fluorescence probe study. [b] Taken from ref 19.

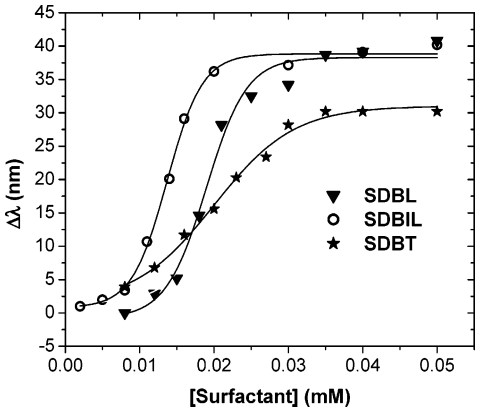

Figure 3. Shift ($\Delta\lambda$) of the emission maximum of NPN versus [surfactant] for SDBL, SDBIL, and SDBT surfactants.

rise in intensity in going from a polar to nonpolar environment.[15] Therefore, the fluorescence emission spectrum of NPN was recorded in the presence of varying concentrations of the surfactants. The shift ($\Delta\lambda$) in emission maximum with respect to water [$\Delta\lambda = \lambda_{max}(\text{water}) - \lambda_{max}(\text{surf})$] was plotted as a function of the surfactant concentration (Figure 3). It is important to note that, at the highest concentration employed, $\Delta\lambda$ for SDBT is lower compared to those for SDBL and SDBIL. The inflection point of the sigmoid plot gave the cac value, which is closer to the corresponding value obtained by surface tension measurement. The cac values of the amphiphiles are much lower than those reported for other NAASs.[16]

Transmission Electron Microscopy. The morphology of the self-assemblies formed by the surfactants was observed under an electron microscope using the negative staining method. The micrographs are shown in Figure 4. Closed spherical vesicles were observed in dilute (0.125 mM) aqueous solutions of SDBL (A), SDBIL (C), and SDBT (D). In concentrated solutions (1 mM) tubules were observed along with the vesicles. The tubule obtained for 1 mM SDBL is shown in image B. The tubules are probably formed by the fusion of vesicles with an increase of the surfactant concentration. The vesicles of SDBL and SDBIL have outer diameters in the range of 100−170 nm. On the other hand, the size of the vesicles (150−500 nm) of SDBT is bigger than that of the vesicles of SDBL and SDBIL. From the TEM pictures it is not possible to comment on whether the vesicles are unilamellar or multilamellar. Images E and F of Figure 4 show the micrographs obtained for 0.125 mM SDBL in 50 mM borate buffer, pH 9.7. These micrographs clearly show that vesicles are formed in aqueous solutions of high ionic strength and pH.

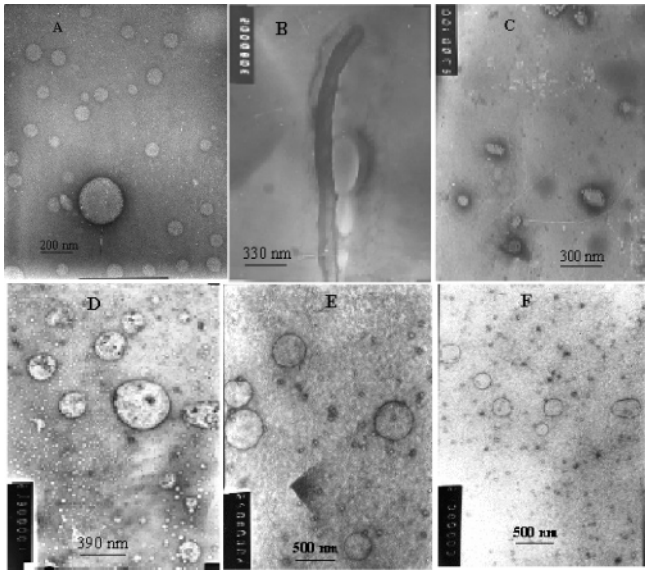

Figure 4. Negatively stained transmission electron micrographs of 0.125 mM SDBL (A), SDBIL (C), and SDBT (D) and 1 mM SDBL (B) in water and 0.125 mM SDBL in 50 mM borate buffer, pH 9.7 (E, F).

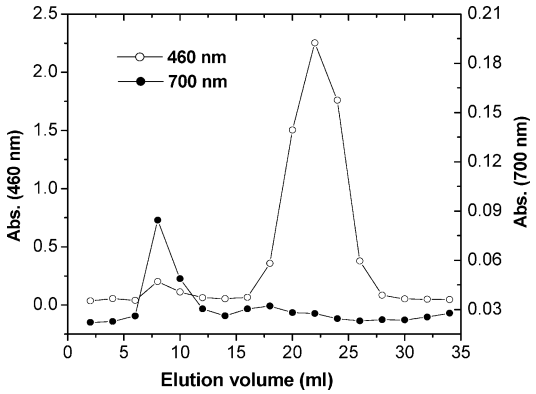

Figure 5. Gel permeation chromatographic separation of SDBL vesicles containing methyl orange (peak 1) from free, nonentrapped methyl orange (peak 2). The absorbance of methyl orange at 460 nm and turbidity at 700 nm due to scattering of light by the large vesicles were recorded as a function of the elution volume.

Trapping Experiments. To prove the existence of an aqueous cavity inside the vesicles, dye-trapping experiments (see the Experimental Section) were carried out using methyl orange as the dye for all the amphiphiles as suggested by Walde and coworkers.[17] The water-soluble dye entrapped inside the vesicles and the free, nonentrapped dye were separated by gel permeation chromatography (GPC) using Sepharose 4B as the column matrix. The representative GPC elution profile obtained for SDBL vesicles is shown in Figure 5. The first peak in Figure 5 corresponds to the entrapped dye, and the second peak corresponds to the free, nonentrapped dye.

Dynamic Light Scattering (DLS) Studies. DLS measurements were performed to determine the *z*-average diameter (D_z) of the vesicles formed by the amphiphiles. Results obtained for all the amphiphiles at a concentration of 0.125 mM are included in Table 1. The size distribution (not shown here) of the vesicles was found to be monomodal with a relatively low polydispersity index, PDI (0.12−0.26), indicating formation of aggregates of uniform size. The large D_z values are consistent with the formation of spherical vesicles shown by the TEM pictures.

(15) Cehelnik, E. D.; Cundall, J. R.; Lockwood, J. R.; Palmer, T. F. *J. Phys. Chem.* **1975**, *79*, 1369.
(16) Miyagishi, S.; Asakawa, T.; Nishida, M. *J. Colloid Interface Sci.* **1989**, *131*, 68.
(17) Namani, T.; Walde, P. *Langmuir* **2005**, *21*, 6210.

Microenvironment of the Self-Assemblies. The micropolarity of the self-assemblies was measured using pyrene as the fluorescence probe. The polarity ratio, I_1/I_3, was measured for all the amphiphiles at a concentration of 0.5 mM (Table 1). The value of I_1/I_3 is very low compared to that in water (1.71), which indicates that pyrene is solubilized in the hydrophobic region of the self-assemblies.[18] Such a highly nonpolar microenvironment is consistent with the formation of bilayer aggregates. The I_1/I_3 value is the same for all three surfactants within the limit of experimental error. This is because pyrene is solubilized deep into the hydrocarbon region of the bilayer. However, the micropolarity of the bilayer interface as indicated by the $\Delta\lambda$ values of the NPN probe is higher in the case of SDBT as compared to SDBL and SDBIL. The low polarity of the hydrocarbon region of the bilayer vesicles is consistent with the high values of the microviscosity (η_m) of the vesicles formed by SDBL and SDBIL.[19] The microviscosity in the case of SDBT vesicles was also determined using 1,6-diphenyl-1,3,5-hexatriene (DPH) as the probe molecule. Steady-state fluorescence anisotropy, r (0.195), and fluorescence lifetime, τ_f (7.05 ns), values of DPH in the presence of the SDBT amphiphile were measured to obtain the η_m value (see Table 1) using the procedure described in our earlier work.[19] The η_m values of the three amphiphiles are equal within the experimental error limit. This is because the structures of the amphiphiles are similar and the probe molecule is solubilized in the hydrocarbon region of the bilayer. However, the η_m values of these amphiphiles are much higher compared to that in micellar structures.[20] As argued in our earlier paper, the increased viscosity (i.e., rigidity) of the microenvironment is due to the tight packing of the hydrocarbon chains of the amphiphilic molecules in the bilayer aggregate.

^{1}H NMR Spectra. ^{1}H NMR spectroscopic measurements were performed to understand the nature of the molecular interactions that are responsible for the tight packing of the amphiphilic molecules in the bilayer self-assemblies. The molecular structures of all the surfactants used in this study are similar. Consequently, similar molecular interactions are expected to occur in all the cases. Therefore, as a representative example, the ^{1}H NMR spectrum of *N*-[4-(*n*-dodecyloxy)benzoy]-L-leucine was recorded in $CDCl_3$ at two different concentrations. The ^{1}H NMR spectrum (see Figure S3 of the Supporting Information) shows a remarkable difference at two different concentrations. The peak for the CON*H* proton is shifted from 6.51 ppm at 5 mM to 6.70 ppm at 150 mM *N*-[4-(*n*-dodecyloxy)benzoyl]-L-leucine in $CDCl_3$ solvent, indicating that the amide proton is strongly hydrogen bonded in concentrated solution. The molecular structure of SDBL shows that there can be stable intermolecular hydrogen bonding (HB) between NH and CO in the amide group that induces a stable linear state. The intermolecular amide HB has also been reported for many NAASs.[21] The intermolecular HB interaction between amide groups in SDBL, SDBIL, and SDBT along with the $\pi-\pi$ stacking interaction between benzene rings results in a layer structure (see Chart 2). Although there is a possibility of formation of amide−water HB in aqueous surfactant solutions, which can reduce the strength of amide−amide intermolecular HB, the expulsion of water molecules from the self-assemblies (indicated by low polarity sensed by the NPN and pyrene probes) makes the way for formation of strong intermolecular amide−amide hydrogen bonds.

Chart 2. Schematic Diagram of the Bilayer Structure Formed by SDBL, SDBIL, and SDBT Amphiphiles

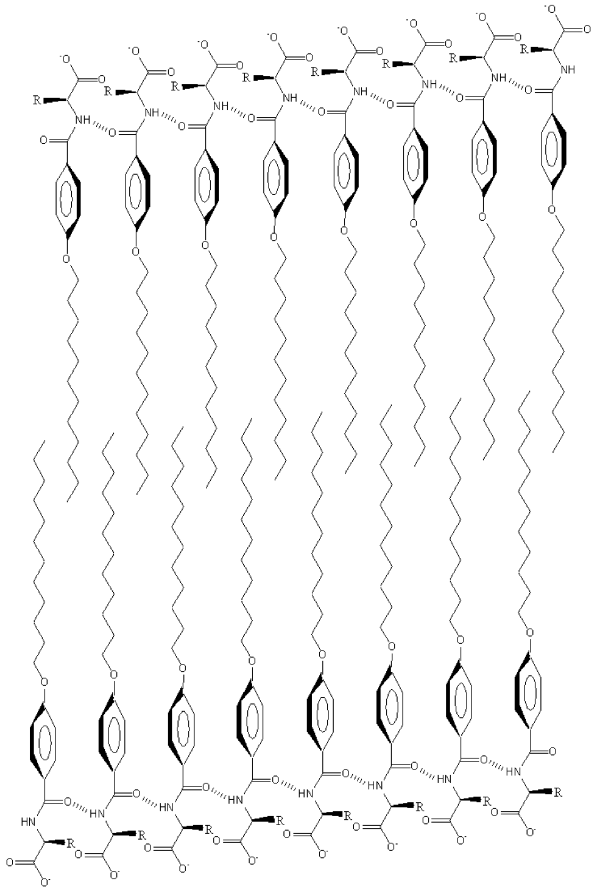

Circular Dichroism Spectra. In the literature, it has been suggested that the presence of chiral centers at the surfactant headgroup can lead to twisting of the bilayer structures, resulting in formation of helical ribbons and/or strands, tubules, and rodlike aggregates.[22] In fact, we have also demonstrated formation of such aggregates by the structurally similar amphiphile SDBV.[12b] SDBL has one chiral center, and both SDBIL and SDBT have two chiral centers near the polar headgroup. Therefore, circular dichroism (CD) spectra of the surfactants were recorded in aqueous solution at concentrations above their respective cac value to examine whether chiral aggregate formation occurs due to self-association of the surfactant monomers. The spectra recorded for 0.5 mM SDBL, SDBIL, and SDBT solutions are depicted in Figure 6. The CD spectrum measured below the cac of SDBL is also included in the figure for discussion. At concentrations above the cac, the CD spectra in water exhibit three bands at 200, 215, and 250 nm. A band at 225 nm also appears as a shoulder to the 215 nm band. The band at 250 nm is due to the electronic absorption of the aromatic ring. The appearance of CD bands in the range 200−240 nm suggests formation of helical aggregates in water. The intensity of the bands decreases as the concentration of the surfactants decreases, and finally, the bands disappear at concentrations below the cac value. The disappearance of the CD band systems at a

(18) (a) Shinitzky, M.; Dianoux, A. C.; Itler, C.; Weber, G. *Biochemistry* **1971**, *10*, 2106. (b) Shinitzky, M.; Yuli, I. *Chem. Phys. Lipids* **1982**, *30*, 261.
(19) Roy, S.; Mohanty, A.; Dey, J. *Chem. Phys. Lett.* **2005**, *414*, 23.
(20) Christov, N. C.; Denkov, N. D.; Kralchevsky, P. A.; Broze, G.; Mehreteab, A. *Langmuir* **2002**, *18*, 7880.
(21) (a) Du, X.; Hlady, V. *J. Phys. Chem. B* **2002**, *106*, 7295. (b) Boettcher, C.; Schade, B.; Fuhrhop, J. H. *Langmuir* **2001**, *17*, 873. (c) Imae, T.; Takahashi, Y.; Muramatsu, H. *J. Am. Chem. Soc.* **1992**, *114*, 3414. (d) Shinitzky, M.; Haimovitz, R. *J. Am. Chem. Soc.* **1993**, *115*, 12545. (e) Song, J.; Cheng, Q.; Kopta, S.; Stevens, R. *J. Am. Chem. Soc.* **2001**, *123*, 3205. (f) Bhattacharyya, S.; Krishnan-Ghosh, Y. *J. Chem. Soc., Chem. Commun.* **2001**, 185.
(22) (a) Nandi, N.; Bagchi, B. *J. Am. Chem. Soc.* **1996**, *118*, 11208. (b) Roy, S.; Das, D.; Dasgupta, A.; Mitra, R. N.; Das, P. K. *Langmuir* **2005**, *21*, 10398.

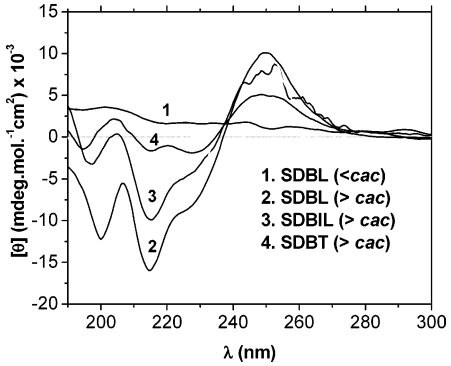

Figure 6. Circular dichroism spectra of 0.01 mM SDBL (1) and 0.5 mM SDBL (2), SDBIL (3), and SDBT (4) in water.

concentration below the cac suggests that the chiral structure is formed through aggregation. It is interesting to note that the molar ellipticity of the bands decreases in the order SDBL > SDBIL > SDBT. This must be due to the presence of a second stereogenic center in the amino acid side chain of SDBIL and SDBT that hinders twisting of the bilayer aggregates. In addition to the spatial orientation of the two stereogenic centers, the changes in electrostatic interactions originated from the varying headgroup structures of the amphiphiles may also play an important role in determining the chirality of the aggregate domain, as suggested by Thirumoorthy et al.[23]

Stability of the Self-Assemblies. The stability of vesicles is an important issue as far as drug delivery is concerned. The experimental results described so far indicate the formation of bilayer vesicles in dilute aqueous solutions of the surfactants. It is well-known that the morphology of the aggregates formed by surfactant molecules changes with aging and a change of conditions such as the surfactant concentration, ionic strength, pH, and temperature.[24] Therefore, the influence of these variables was investigated. The effect of the surfactant concentration was studied by measuring the concentration dependence of the fluorescence anisotropy (r) of DPH in the presence of all three surfactants. The r value decreased with an increase of the surfactant concentration (see Figure S4 of the Supporting Information), indicating loose packing of the surfactant monomers in the self-assemblies. However, the decrease of the r value is smaller in the case of SDBT compared to that of SDBL and SDBIL. The sigmoid nature of the plots suggests a reversible transition between two states. The effect of the surfactant concentration was further evaluated by performing DLS measurements at different concentrations of the amphiphile in the range from 0.05 to 2 mM in 20 mM phosphate buffer, pH 7.2. The results suggest that spherical vesicles of relatively uniform size (indicated by low PDI values) are formed just after the cac and at low surfactant concentrations (0.05−0.25 mM). A further increase of the surfactant concentration up to 1 mM has very little impact on the *z*-average size, but the PDI value increases gradually with an increase of the surfactant concentration, suggesting formation of other types of aggregates, i.e., elongated vesicles and tubules, possibly due to the fusion of spherical vesicles. Indeed, an increase of the surfactant concentration to 2 mM results in a bimodal distribution of the particle sizes for both SDBL and SDBIL. A representative plot showing the effect of the SDBL concentration on the particle size distribution is shown in Figure 7. This was also accompanied by a decrease of

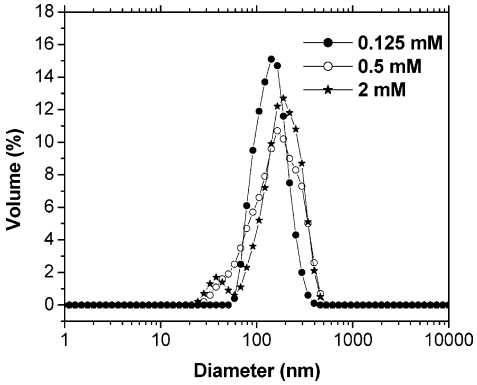

Figure 7. Particle size distribution at different SDBL concentrations measured in 20 mM phosphate buffer, pH 7.2.

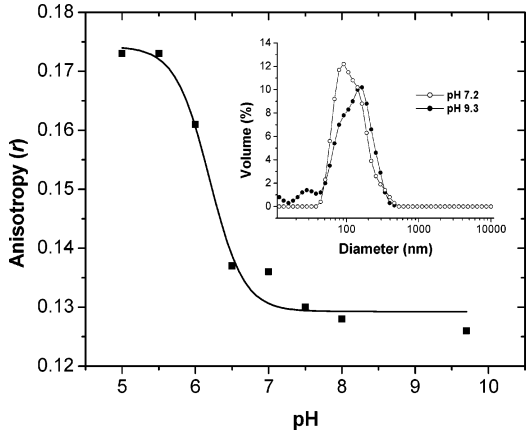

Figure 8. Variation of the fluorescence anisotropy (r) of DPH with pH in the presence of 0.125 mM SDBT. Inset: Particle size distribution of 0.125 mM SDBT at pH 7.2 and 9.3.

the ζ potential from −56.2 to −35.5 mV for SDBL and from −60.4 to −38.2 mV for SDBIL. The existence of rodlike microstructures in the TEM micrographs corresponding to the sample containing 1 mM SDBL is shown in Figure 4. However, DLS measurements for SDBT solutions in the entire concentration range from 0.05 to 2 mM give a monomodal distribution with a relatively low PDI (0.256) value. This suggests that the vesicles of SDBT are more stable in this concentration range, which may be due to HB interaction of the −OH group at the amino acid side chain.

The surfactants being sodium salts of carboxylic acids, it is important to check the effect of the pH on the aggregation behavior of the amphiphiles. This is because the pH-induced protonation of the carboxylate ion affects the hydrophilic interaction between the headgroups of the ionic surfactants and hence has a defining effect on the shape and size of the aggregates formed by the surfactant molecules. The effect of the pH was monitored by measuring the fluorescence anisotropy of DPH in the presence of 0.125 mM SDBL, SDBIL, and SDBT. The representative result obtained for SDBT is shown in Figure 8. The plot shows a sigmoidal change of r with pH having an inflection point at pH 6.2. At pH < 7.0 the negatively charged carboxylate ions get partially protonated to produce a neutral carboxylic acid group that results in lowering of the ionic repulsions and hence tight packing of the surfactant monomers in the aggregates indicated by the high r values. At pH > 8.0, the surfactants predominantly remain in the anionic form, and ionic repulsion among the carboxylate ions results in relatively loose packing of the hydrophobic tails of the amphiphiles as suggested by the lowering of the r values. The pH value corresponding to the half-

(23) Thirumoorthy, K.; Nandi, N.; Vollhardt, D. *J. Phys. Chem. B* **2005**, *109*, 10820.

(24) (a) Laughlin, R. G. *The Aqueous Phase Behavior of Surfactants*; Academic Press: London, 1994. (b) Fendler, J. H. *Membrane Mimetic Chemistry*; Wiley: New York, 1982.

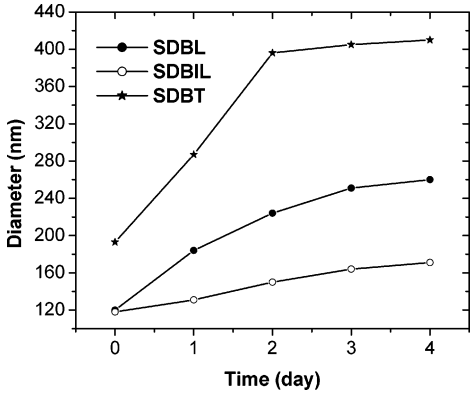

Figure 9. Variation of the vesicle size with aging for SDBL, SDBIL, and SDBT surfactants.

neutralization point (degree of dissociation, $\alpha = 0.5$) of the plot in Figure 8 was taken as the pK_a ($\alpha = 0.5$) of the surfactant aggregates. The pK_a values thus obtained for the amphiphiles are summarized in Table 1. It should be noted that the pK_a values obtained for these carboxylate surfactants in aggregate form are considerably higher than the pK_a of the simple fatty acids.[25] This is not surprising considering the fact that the negative charge density at the surface of the aggregates is considerably high, which can alter the pK_a value. The *r* value for all three surfactants decreases with an increase of the pH. However, the minimum *r* value obtained at higher pH (0.123 at pH 9.7 for SDBT) is still large enough for an ionic surfactant to rule out the possibility of formation of normal spherical micelles. Indeed, the measured *r* value for the micelles of an anionic surfactant, sodium dodecylbenzenesulfonate, is 0.064. The existence of spherical vesicles at pH 9.7 is already shown for SDBL in Figure 4. The decrease in the *r* value is due to relatively loose packing of the surfactant monomers. The loose packing may lead to formation of elongated vesicles or tubules at higher pH values, which coexist along with the vesicles. This is further confirmed by the DLS measurements performed for 0.125 mM SDBL, SDBIL, and SDBT samples at pH 7.2 and 9.3. The DLS results show that both the particle size and PDI increase with an increase of the pH. The loose packing of the surfactant monomers at alkaline pH, as discussed earlier, leads to a slight increase in vesicle size and facilitates deformation of the spherical vesicles to elongated vesicles and tubules. The coexistence of different types of aggregates is indicated by the higher PDI values. Among the three surfactants studied, SDBT vesicles are less stable at higher pH compared to SDBL and SDBIL vesicles. Indeed, the particle size distribution for 0.125 mM SDBT at pH 9.3 gives a bimodal distribution having particles of diameters in the ranges 10−20 and 120−250 nm in contrast to the monomodal distribution obtained at pH 7.2 (see the inset of Figure 8).

DLS measurements and fluorescence probe studies were also performed to check the stability of the vesicles in the temperature range 20−60 °C (results not shown here). Both the studies indicate that the vesicles are stable in this temperature range. The *r* value decreased linearly with an increase of temperature without any phase transition in the studied temperature range as indicated by the absence of any inflection point in the plot of *r* versus temperature (see Figure S5 of the Supporting Information). The decrease of the *r* value can be correlated to the increase in chain mobility in the bilayer vesicles as a result of conformational changes of the hydrocarbon chains.

The stability of the vesicles with aging was investigated by measuring the vesicle size in 20 mM phosphate buffer, pH 7.2, at different intervals of time. The vesicle size increases with time and reaches a plateau after 4−5 days (Figure 9). No further change was observed thereafter, suggesting formation of a stable vesicle phase.

(25) Ireland, J. F.; Wyatt, P. A. H. *Adv. Phys. Org. Chem.* **1976**, *12*, 169.

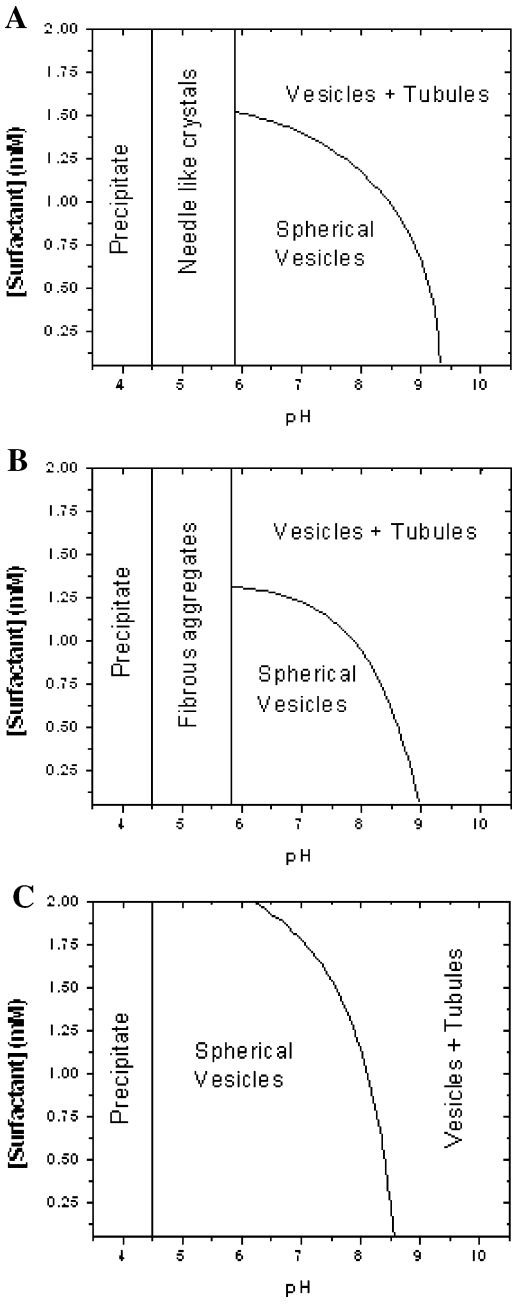

Figure 10. Phase diagram of the water/amphiphile binary systems: (A) SDBL, (B) SDBIL, and (C) SDBT.

Discussion

On the basis of the experimental results, the general phase behavior of the water/amphiphile binary system for all three amphiphiles under investigation is presented in Figure 10. Although structurally similar, the phase diagrams of the three amphiphiles are quite different. The differences in the phase behavior can be attributed to the structural differences near the hydrophilic headgroup. SDBL has an isobutyl group, SDBIL has a secondary butyl group, and SDBT has a relatively polar $-CH(OH)CH_3$ group as the amino acid side chain near the headgroup (see Chart 1). Also, SDBL has one stereogenic center, whereas both SDBIL and SDBT have two stereogenic centers.

The bulkiness of the amino acid side chain and the spatial orientation of the stereogenic centers affect the extent of close packing of the amphiphilic molecules during aggregate formation. This acts as a retarding force for formation of large fibrous aggregates in the low pH region in which partially protonated SDBL molecules get precipitated. The presence of the hydrophilic OH group in SDBT, on the other hand, increases its solubility and formation of vesicles even in a slightly acidic pH. The effect of the stereogenic center at the amino acid side chain is clearly shown by the cac values of the amphiphiles. Thus, SDBIL and SDBT, which have two stereogenic centers, have a lower cac value compared to that of SDBL and SDBV, respectively. The spatial orientation of the groups around the two chiral centers perhaps reduces the interionic repulsions. However, the presence of a second stereogenic center has a negative effect on the formation of helical aggregates. Consequently, the molar ellipticity of the CD band in the cases of SDBIL and SDBT is smaller compared to that of SDBL.

Experimental Section

Materials. The surfactants SDBL, SDBIL, and SDBT were synthesized and purified in the laboratory following the reported procedure.[12b,13] The fluorescence probes pyrene, NPN, and DPH were purchased from Sigma-Aldrich and were recrystallized twice from an ethanol−acetone mixture prior to use. The purity of the compounds was checked by measuring the fluorescence excitation and emission spectra at several wavelengths. Uranyl acetate and methyl orange were purchased from Aldrich and were directly used from the bottle. Analytical grade sodium dihydrogen phosphate, disodium hydrogen phosphate, hydrochloric acid, and other organic solvents were procured locally from SRL, Mumbai, India. Sepharose 4B matrix used for GPC was a gift from Dr. A. Maiti, Department of Biotechnology, Indian Institute of Technology, Kharagpur, India.

General Instrumentation. NMR spectra were recorded using a Bruker SEM 200 instrument in $CDCl_3$ solvent using trimethylsilane (TMS) as the internal standard. UV−vis spectra were recorded on a Shimadzu model 1601 spectrophotometer. The CD spectra were measured with a Jasco J-810 spectropolarimeter using a quartz cell with a path length of 2 or 10 mm. The pH measurements were done with a digital pH meter, model pH 5652 (EC India Ltd., Calcutta), using a glass electrode. Distilled water was deionized (resistivity 18.2 MΩ) using a Milli-Q water purification system (Millipore).

Surface Tension Measurements. Surface tension measurements were performed using a torsion balance (S.D. Hurdson & Co., Calcutta) using the Du Nüoy ring method. A stock solution of the surfactants was prepared using deionized water. An aliquot of the stock solution was added to a beaker containing a known volume of water. The solution was stirred gently using a magnetic stirrer, and the surface tension was measured after equilibration for 5 min at room temperature (30 °C). Three measurements were performed for each sample, and the mean γ (mN m^{-1}) value was recorded. The cac was then obtained from the break point of the γ versus log C plot.

Fluorescence Measurements. Steady-state fluorescence experiments were carried out with a SPEX Fluorolog, model FL3-11, spectrofluorometer. The fluorescence anisotropy measurements were performed on a Perkin-Elmer LS-55 luminescence spectrometer equipped with a filter polarizer and a thermostated cell holder. Temperature was controlled using a circulating bath (Thermo Neslab, RTE 7). For solution preparations, a saturated solution of NPN in deionized water was used, and the pyrene and DPH concentrations were kept at 1×10^{-6} M. Pyrene was excited at 335 nm, and emission spectra were recorded in the wavelength range of 350−500 nm. NPN was excited at 340 nm, and emission spectra were recorded in the wavelength range of 360−600 nm. For fluorescence anisotropy measurements in the presence of surfactant vesicles, DPH was excited at 350 nm and the fluorescence intensity was measured at 450 nm. The excitation and emission slit widths were 2.5 and 5 nm, respectively. The fluorescence anisotropy value (r) was calculated by the instrumental software using the equation

$$r = (I_{VV} - GI_{VH})/(I_{VV} + 2GI_{VH}) \quad (1)$$

where I_{VV} and I_{VH} are, respectively, the fluorescence intensities of the emitted light polarized parallel and perpendicular to the excited light and $G = I_{HV}/I_{HH}$ is the instrumental grating factor. The fluorescence measurements were performed at 30 °C if not mentioned otherwise.

Time-Resolved Fluorescence Measurements. Fluorescence lifetimes of the DPH probe were determined from time-resolved intensity decay by the method of time-correlated single-photon counting using a picosecond diode laser at 370 nm (IBH, U.K., nanoLED-07) as the light source. The typical response time of this laser system was 70 ps. The decay was analyzed using IBH DAS-6 decay analysis software. The fluorescence decay curve was analyzed by a biexponential iterative fitting program provided by IBH. The best fit was judged by the χ^2 value (0.8−1.3) and residual plot.

Light Scattering Measurements. A Zetasizer Nano ZS light scattering apparatus (Malvern Instruments, U.K.) with a He−Ne laser (633 nm, 4 mW) was used for DLS measurements. The Nano ZS instrument incorporates noninvasive backscatter (NIBS) optics with a detection angle of 173°. The *z*-average diameter and the PDI of the samples were automatically provided by the instrument using cumulant analysis. The size quoted throughout this paper is the *z*-average diameter. For particle size measurements, a surfactant solution of appropriate concentration was made in Milli-Q water and was filtered directly into the quartz cell using a Millex-GV (Millipore) membrane filter (0.45 μm pore size). The quartz cell was rinsed several times with filtered water and then filled with the filtered sample solution. The DLS measurements began 5−10 min after the sample cell was placed in the DLS optical system. The data obtained in each case are the average of 50 runs, each run of 10 s duration. The temperature was maintained at 30 °C.

ζ Potential Measurements. The ζ potential of the vesicles was measured with a Zetasizer Nano ZS instrument (Malvern Instruments Ltd., U.K.) using disposable polystyrene folded capillary cells. The instrument calculates the ζ potential by measuring the electrophoretic mobility (μ_e) using the laser Doppler velocimetry (LDV) technique and then applying the Henry equation[26]

$$\mu_e = 2\epsilon\zeta[f(ka)]/3\eta \quad (2)$$

where ϵ is the dielectric constant, η the viscosity, and $f(ka)$ the Henry function. The value of $f(ka)$ was taken as 1.5 according to the Smoluchowski approximation[27] for aqueous solutions. The samples were made in 20 mM phosphate buffer, pH 7.2, and were injected into the cell by a syringe to avoid generation of bubbles inside the cell. For each sample the ζ potential was measured five times, each measurement consisting of 50 runs, and then the average ζ potential value was recorded.

Optical and Electron Microscopy. Optical micrographs were obtained from a Leica-DMRXP microscope. The images taken by the video camera were analyzed by Leica Qwin software. The surfactant solution containing the fibrous aggregates was placed on a glass slide and viewed through the microscope. A Philips CM 200 electron microscope operating at a voltage of 120 kV was used for TEM measurements. The surfactant solutions were filtered through a Millex-GV (Millipore) membrane filter of 0.45 μm pore size. A drop of the surfactant solution was placed on the carbon-coated copper grid and was allowed to stand for 2 min. The excess solution was blotted off with filter paper followed by staining with 2% aqueous uranyl acetate solution. The specimens were then dried in a desiccator until before the measurement.

Dye Trapping Experiment. A Sepharose 4B column of 25 cm height and 1.2 cm diameter was used to separate the highly water soluble dye methyl orange entrapped inside the vesicle from the

(26) Hunter, R. J. *Zeta Potential in Colloid Science, Principles and Applications*; Academic Press: London, 1981.

(27) Von Smoluchowski, M. Z. *Phys. Chem.* **1918**, *44*, 1.

free, nonentrapped dye in bulk solution using gel permeation chromatography. A stock solution of 2 mM methyl orange was prepared in 2 mM surfactant solution and was allowed to stand for 1 h. A 0.5 mL sample of the stock solution was introduced into the column and was eluted with deionized water. The eluent was collected in 2 mL fractions, and the absorbance of each fraction was measured at both 460 nm (absorbance maximum of methyl orange) and 700 nm (for turbidity of the vesicles). Finally, the chromatogram was constructed by plotting the elution volume versus absorbance.

Acknowledgment. This work was supported by CSIR (Grant No. 05(1664)/00/EMR-II), New Delhi.

Supporting Information Available: UV−vis spectra, turbidity studies, ^{1}H NMR spectra showing the hydrogen bonding among the amphiphile molecules, and the surfactant concentration and temperature dependence of the fluorescence anisotropy of DPH. This material is available free of charge via the Internet at http://pubs.acs.org.

LA0625143